Redox Biology 59 (2023) 102573

Contents lists available at ScienceDirect

Redox Biology

journal homepage: www.elsevier.com/locate/redox

The mechanism and significance of the conversion of xanthine dehydrogenase to xanthine oxidase in mammalian secretory gland cells

Teruo Kusano [a], Tomoko Nishino [a], Ken Okamoto [a,1], Russ Hille [b], Takeshi Nishino [a,*,1]

[a] Department of Biochemistry and Molecular Biology, Nippon Medical School, 1-1-5, Sendagi, Bunkyo-Ku, Tokyo, Japan
[b] Department of Biochemistry, University of California, Riverside, USA

A B S T R A C T

The conversion of xanthine dehydrogenase (XDH) to xanthine oxidase (XO) occurs only in mammalian species. In fresh bovine milk, the enzyme exists predominantly as the oxidase form, in contrast to various normal organs where it is found primarily as the dehydrogenase: the mechanism of conversion to the oxidase in milk remains obscure. A systematic search for the essential factors for conversion from XDH to XO has been performed within fresh bovine milk using the highly purified dehydrogenase form after removal endogenous oxidase form by fractionation analysis. We find that conversion to the oxidase form requires four components under air: lactoperoxidase (LPO), XDH, SCN^-, and substrate hypoxanthine or xanthine; the contribution of sulfhydryl oxidase appears to be minor. Disulfide bond formation between Cys-535 and Cys-995 is principally involved in the conversion, consistent with the result obtained from previous work with transgenic mice. *In vitro* reconstitution of LPO and SCN^- results in synergistic conversion of the dehydrogenase to the oxidase the presence of xanthine, indicating the conversion is autocatalytic. Milk from an LPO knockout mouse contains a significantly greater proportion of the dehydrogenase form of the enzyme, although some oxidase form is also present, indicating that LPO contributes principally to the conversion, but that sulfhydryl oxidase (SO) may also be involved to a minor extent. All the components XDH/LPO/SCN^- are necessary to inhibit bacterial growth in the presence of xanthine through disulfide bond formation in bacterial protein(s) required for replication, as part of an innate immunity system in mammals. Human GTEx Data suggest that mRNA of XDH and LPO are highly co-expressed in the salivary gland, mammary gland, mucosa of the airway and lung alveoli, and we have confirmed these human GTEx Data experimentally in mice. We discuss the possible roles of these components in the propagation of SARS-CoV-2 in these human cell types.

1. Introduction

Milk contains high levels of xanthine oxidase, XO [1,2]. Historically, the enzyme was first isolated from bovine milk as an aldehyde oxidase in 1902 [3] and subsequently shown to be identical to the xanthine-oxidizing enzyme in 1926 [4]. The enzyme was subsequently found in other mammalian tissues [5], notably as interconvertible dehydrogenase and oxidase forms in rat liver [6,7] supernatant [8], where it catalyzed the oxidative hydroxylation of hypoxanthine and xanthine to uric acid with concomitant reduction of NAD^+ in the case of the dehydrogenase form or molecular oxygen as the oxidase form. Similar to the rat liver dehydrogenase [9], the bovine dehydrogenase can reduce molecular oxygen in the absence of NAD^+, albeit much less effectively than the oxidase form [10]. On the other hand, the oxidase form of the enzyme cannot reduce NAD^+ at all [9,10]. The dehydrogenase and oxidase forms are products of the same gene and are interconvertible by disulfide formation between specific cysteine amino acid residues or by proteolytic cleavage [11]. Interestingly, the conversion of the dehydrogenase to the oxidase – the so-called D→O conversion – occurs only in mammals; other organisms, from chicken to bacteria, have obligatory dehydrogenases that cannot be converted to an oxidase form [11]. Thus, the mammalian enzyme has attracted much attention for over a century not only from the standpoint of its fundamental enzymology including the structural basis of the D→O conversion [12], but also because of its role in the generation of uric acid and reactive oxygen species (ROS; H_2O_2 and $O_2^{\bullet-}$) in the oxidase form [13,14]. Inhibitors of the enzyme are commonly used in the treatment of gout to decrease hyperuricemia associated with a range of pathological conditions.

Although the D→O conversion in the mammalian enzyme is well understood to arise from either disulfide formation or by hydrolysis of specific peptide bonds in the protein [15], it remains unclear as to why the predominant form found in milk is the oxidase, even when extreme care is taken to avoid proteolysis in the course of purification [16]. A variety of possible roles for the oxidase form have been proposed over the years, including: (1) filling the nutritional needs of the neonate [17]; (2) contributing to innate immunity defense from infection [18]; and (3)

Abbreviations: D→D conversion, xanthine dehydrogenase to xanthine oxidase conversion.

* Corresponding author. Department of Biochemistry and Molecular Biology, Nippon Medical School, 1-1-5, Sendagi, Bunkyo-Ku, Tokyo, Japan.
E-mail address: nishino@nms.ac.jp (T. Nishino).
[1] Department of Applied Biological Chemistry, Graduate School of Agricultural and Life Sciences, The University of Tokyo, 1-1-1, Yayoi, Bunkyo-ku, Tokyo, Japan

https://doi.org/10.1016/j.redox.2022.102573
Received 4 November 2022; Received in revised form 3 December 2022; Accepted 5 December 2022
Available online 9 December 2022

involvement in fat droplet secretion accompanying lactation due to conformational changes rather than activity [19] (The human enzyme from milk exhibits low activity due to defective formation of a functional molybdenum center in the active site [20]). Transgenic mouse lines in which the wild-type enzyme has been replaced by stable dehydrogenase or oxidase forms exhibit normal lactation, and no particular phenotype has been observed under normal life conditions [21]. A recent review of our current understanding has led to the conclusion that the D→O conversion most likely plays a role in innate immunity [22], but it remains unclear what specific role the conversion might play. It has been reported that there is a sulfhydryl oxidase (SO) activity in bovine milk [23], and a second report has suggested that SO, in combination with LPO, can catalyze the D→O conversion (LPO) [24]. However, these reports showed SO activity using only a model compound as substrate and did not directly determine the extent of the D→O conversion. Further complicating interpretation, xanthine dehydrogenase (XDH) and LPO are secreted into milk from different mammary gland cell types and come together only after lactation.

To better understand the mechanistic and physiological role of the D→O conversion in the mammary gland, we have examined the process in fresh bovine milk using purified re-convertible XOR protein and transgenic mice analyses. We find the conversion is autocatalytic and requires four specific components: LPO, SCN^-, a reducing substrate such as xanthine and the dehydrogenase itself; SO is minimally involved in the conversion. We discuss the possible role of this system in the propagation of SARS-CoV-2 in secretory and pulmonary tissue.

2. Materials and methods (Experimental procedures)

2.1. Animals

LPO gene-modified mice were produced at Nippon Medical School. The mouse LPO knock-out was designated C57BL/6-*LPO*$^{tm1/Nms}$, abbreviated LPO-ko. The details of the LPO-ko mice are described as below. The stable XDH mouse mutant knock-in (XDH-ki) was constructed as described elsewhere [21]. WT, LPO-ko, and XDH-ki mice, all in the C57BL/6J background, were age- and sex-matched in the different experimental settings. Unless otherwise stated, mice were used between 8–24 weeks old. All *in vivo* experimental protocols were approved by the institutional animal care committees of the Nippon Medical School, and extreme care was taken throughout the study to minimize animal pain and discomfort, and without infection experiments.

2.2. Materials

ß-NAD^+ (grade V–C), 4,4′-dithiodipyridine (4-DPS), lactoperoxidase (E.C. 1.11.1.17, 80–150 units/mg protein, A412/A280 = 0.88–0.95), Horseradish peroxidase (Type XII, E.C. 1.11.1.17, 285 units/mg protein, A403/A275 = 3.3), 2,2′-azino-bis (3-ethylbenzothiazoline-6-sulfonic acid) (ABTS) and xanthine were obtained from Sigma Chemical Co. (St. Louis, MO). Dithiothreitol (DTT) was purchased from Wako Pure Chemical Industries, Ltd. (Osaka, Japan). Rennin (calf stomach, E.C. 3.4.23.4) was obtained from ICN Biomedicals Inc. (Irvine, CA). Activity flavin ratio (AFR), the specific activity of XOR, is measured as the ratio of urate formation activity (ΔA295/nm) to A450 (absorbance of the enzyme in the reaction mixture). Bovine milk XOR (AFR more than 150) was prepared by following the procedure of Nishino et al. [25] but omitting the second folate affinity chromatography step. Three variants of rat liver XOR, C535A/C992R, C535A/C992R/C1324S, and C535A/C992R/C1316S were constructed and purified as described elsewhere [26]. The dehydrogenase form of these enzymes was purified in the presence of DTT. Purified XORs were treated with 5 mM DTT for 1 h at 25 °C and then passed through a Sephadex G-25 column to remove excess DTT immediately prior to use. The ratio of dehydrogenase to oxidase activity (D/O) was determined as the ratio of the absorbance change at 295 nm under aerobic conditions in the presence of NAD^+ to that in the absence of NAD^+, as defined by Waud and Rajagopalan [27]. The bovine milk XDH sample used in this study had a D/O ratio of greater than 5, indicating that it was mostly in the dehydrogenase form. The XO form was prepared by chemical modification of cysteine residues with 4-DPS for 1 h at 25 °C, and then passed through a Sephadex G-25 column to remove excess 4-DPS immediately prior to use. Thiocyanate hydrolase was generously provided by Dr. M. Odaka (Tokyo University of Agriculture and Technology, Tokyo, Japan). All other chemicals and reagents were of reagent grade and were obtained from either Sigma Chemical Co. or Wako Pure Chemical Industries. TOYOPEAL SuperQ-650C, and TOYOPEAL CM-650 M were obtained from TOSHO Corporation (Tokyo, Japan). Macro-Prep Ceramic Hydroxyapatite Type I was from Bio-Rad Laboratories, Inc. (Hercules, CA). Polyvinylidene difluoride membrane (FluoroTrans) was purchased from Pall Corporation (Ann Arbor, MI). Superose 6 HR 10/30, Sephadex G-10 (fine), and Sephadex G-25 (fine) were purchased from GE Healthcare Bio-Science Corp. (Piscataway, NJ). Ultrafiltration membranes and Amicon Centricon-10 concentrator were purchased from Millipore Corporation (Bedford, MA). Deionized water (18 MΩ cm) that was drawn from a Milli-Q system (Millipore) was used throughout this work for solution of all reagents and in all steps of enzyme purification.

2.3. Xanthine oxidoreductase activity assay

For rodent XOR, activity assays were performed in 50 mM potassium phosphate buffer, pH 7.8, 0.4 mM EDTA under aerobic conditions at 25 °C. In the case of the bovine XOR, 0.1 M pyrophosphate buffer, pH 8.5, 0.2 mM EDTA, was used as a buffer solution. XDH activity was determined by following the NAD^+-dependent oxidation of xanthine, which was monitored by the increase in absorbance at 340 nm due to the accumulation of NADH (6220 M^{-1} cm^{-1}). The reaction medium consisted 150 μM xanthine and 0.5 mM ß-NAD^+ within buffer solution. The appearance of NADH was measured after addition of 20 nM (final concentration) of purified XOR to the reaction medium. In the case of milk or tissue lysate assay, sample was added to the reaction mixture to 1–3% (final concentration). The rate of product formation was determined from the initial linear rate of increased absorbance. Total activity was determined by following the NAD^+ plus O_2-dependent oxidation of xanthine, which was monitored by measuring the increase in absorbance at 295 nm due to the accumulation of uric acid (9600 M^{-1} cm^{-1}). The reaction conditions were the same as describe above. XO activity was determined by following the O_2-dependent oxidation of xanthine to uric acid. The reaction condition was the same as describe above without NAD^+ in the reaction mixture.

2.4. D→O activity assay

Exogenously purified XDH was incubated with bovine milk fractions in 50 mM sodium phosphate buffer pH 7.0 at 25 °C. The final concentrations of XDH, Fraction L, Fraction S, LPO, horseradish peroxidase (HRP), NaSCN, and H_2O_2 in the assay mixture were 2 μM, 1%, 40%, 20 nM, 20 nM, 16 μM, and 0.1 mM, respectively. Combination of each component was performed as described in figure legends. Aliquots were withdrawn after incubation at appropriate time intervals, and diluted 100-fold (corresponding to 20 nM of XOR) into the XOR assay reaction medium as described above to stop the D→O reaction. XOR activity was measured immediately after dilution. D→O activity was assessed by the increased XO activity, assayed as described above.

2.5. Peroxidase activity assay

Peroxidase activity was determined with ABTS as a reducing substrate [28], monitoring formation of ABTS radical cation at 414 nm (36.8 mM^{-1} cm^{-1}). Assay conditions were: 0.5 mM ABTS, 0.15 mM H_2O_2, 50 mM sodium phosphate buffer, pH 7. Assay was performed under aerobic conditions at 25 °C.

2.6. Processing and fractionation of bovine milk

Fresh, raw, unprocessed bovine milk was obtained from a local dairy. Skim milk was prepared from this by centrifugation at 10,000×*g* for 10 min at 4 °C. The skim milk thus obtained was treated with rennin (2 mg per 100 ml of skim milk) for 30 min at 30 °C and the resulting insoluble curd removed by centrifugation at 10,000×*g* for 30 min at 4 °C. The supernatant fraction (whey) was fractionated by an ultrafiltration system (Amicon Model 8200, Millipore) using a 100-kDa exclusion membrane (YM100) and the filtrate further fractionated using a 30-kDa exclusion ultrafiltration membrane (YM30). The concentrated fraction thus obtained, the large molecular weight fraction (Fraction L), was then equilibrated with 50 mM sodium phosphate buffer (pH 8) by diafiltration against a 200-fold volume of buffer solution. The fraction passing through the YM30 membrane, designated the small molecular weight fraction (Fraction S), was used as an activator for the D→O assay.

2.7. Purification of the protein component of the D→O activity

Details of the purification procedure using anion exchange, cation exchange, and hydroxyapatite chromatography are described in Supplementary Figure S1. For the final step in the purification, the crude protein component of the D→O activity was applied to a gel-filtration column (Superose 6 HR 10/30; 1 cm × 30 cm) that had been equilibrated with 50 mM sodium phosphate buffer (pH 7.0), containing 200 mM sodium chloride. The protein component of the D→O activity was eluted with the same buffer at a flow rate of 1.0 ml/min. Calibration of the column was carried out with carbonic anhydrase *(Mr,* 29,000), bovine serum albumin (*Mr*, 66,000), sweet potato ß-amylase (*Mr*, 200,000), and horse spleen apoferritin (*Mr*, 443,000) as molecular weight markers. The molecular weight of the native protein component of the D→O activity was determined by comparing its retention time with those of the authentic standards. Fractions possessing D→O activity were concentrated by Centricon-10 concentrator and stored on ice.

2.8. Preparation of tissue lysate from mouse tissue

Excised tissues (salivary gland, lung, liver, mammary gland) were constantly treated with ice-cold condition. Freshly excised mouse organ was washed in 0.9% NaCl and suspended in three-fold volume per samples' wet weight of 0.05 M potassium phosphate buffer (pH 7.4) containing 0.25 M sucrose, 1 mM sodium salicylate, and 0.3 mM EDTA. Protease inhibitor cocktail, cOmplete (Roche, Mannheim, Germany), was employed to prevent non-specific proteolytic cleavage of XOR. The tissue suspension was homogenized by a loose-fitting Teflon-glass homogenizer in ice bath. The insoluble fraction was removed from tissue homogenate by centrifugation at 10,000×*g* for 30 min at 4 °C. The supernatant fraction was used as a tissue lysate.

2.9. Protein determination

Total protein concentrations were determined using the dye-binding method of Bradford [29] with a PIERCE kit, using bovine serum albumin as the standard. The concentration of LPO was determined spectrophotometrically using an extinction coefficient of 114,000 M^{-1} cm^{-1} at 412 nm [30]. The concentration of HRP was determined spectrophotometrically using an extinction coefficient of 102,000 M^{-1} cm^{-1} at 402 nm [31]. The concentration of bovine milk XOR and rat liver XOR was determined spectrophotometrically using an extinction coefficient of 37, 800 and 35,800 M^{-1} cm^{-1} at 450 nm, respectively [32,33].

2.10. Electrophoresis

Sodium dodecyl sulfate-polyacrylamide gel electrophoresis (SDS-PAGE) on slab gels was performed using a precast polyacrylamide gel (READY GELS J or Mini-PROTEAN Gel, Bio-Rad Laboratories, CA), according to the method of Laemmli [34]. Mixture of recombinant proteins (Precision Plus Protein Standards, Bio-Rad) was used as a molecular weight standard marker. Gels were stained with silver as described by Oakly et al. [35].

2.11. Western blotting analysis

Proteins resolved on an SDS-PAGE gel were blotted by electrophoretic transfer onto a polyvinylidene fluoride (PVDF) membrane using the Trans-Blot Turbo Blotting System (Bio-Rad). Blotted membranes were washed with 0.05 M Tris-HCl (pH 7.6), 0.15 M NaCl, 0.5% Tween 20 (TBS-T) for 5 min and blocked for 1 h in 5% (w/v) skimmed milk in TBS-T at ambient temperature. Rabbit polyclonal antibodies against rat XOR, bovine XOR, or mouse LPO (laboratory-prepared antibody) were used as primary antibody for rat XOR, bovine XOR and mouse LPO, respectively. HRP-conjugated goat polyclonal anti-rabbit antibody (1:2000, DAKO Cytomation, Glostrup, Denmark) was used as a secondary antibody. The cross-react signals were developed using the ECL Prime reagent (GE Healthcare UK Ltd.) and were visualized by a gel imaging system (ChemiDoc XRS+, Bio-Rad).

2.12. Amino acid sequence analysis

For NH_2 -terminal sequencing, 20 μg of the purified protein component of D→O activity was subjected to SDS-PAGE and electroblotted on a PVDF membrane as described by Matsudaira [36]. The portion of the PVDF membrane containing purified protein component was excised and directly subjected to on-membrane amino acid analysis. Amino acid sequencing was performed by automated Edman degradation using a gas-phase sequencer, model 477A, equipped with PTH analyzer 120A (Applied Biosystems, Foster City, CA).

2.13. Chemical analysis

Thiocyanate concentrations in bovine milk were determined using the method of Sörbo [37].

XOR substrates and uric acid content in bovine milk were determined using a quantitative enzymatic assay (Amplex Red kit, Invitrogen) according to the manufacturer's protocol. Bovine milk was treated with 3% perchloric acid to exclude an effect of milk containing XO and the supernatant neutralized with 0.6 M K_2CO_3 prior to analysis. The results were standardized by using a commercial hypoxanthine, xanthine, and uric acid. XOR substrates were expressed as the amount equivalent to xanthine.

Total sullhydryl content was quantified by a modification of the Ellman's method [38]. Sulhydryl samples (0.08 ml) were added to 25 μM 5,5′-Dithiobis (2-nitrobenzoic acid) (DTNB), 0.1 M pyrophosphate buffer (pH8.5), 0.2 mM EDTA to give a final volume of 0.8 ml, and absorbance was measured at 412 nm. Sulfhydryl concentrations were calculated using a molar extinction of 13,600 M^{-1} cm^{-1} for 5-Mercapto-2-nitrobenzoic acid (product of reduced DTNB).

2.14. Construction of LPO ko

LPO-deficient mice were generated from C57BL/6 mice by replacing the *Sac* I segment (4535–7113) containing Exon 2 and Exon 3 of the LPO gene with a neomycin resistance gene (*neo*^{r}) (Suppl. Fig. 3). A diphtheriae toxin A subunit (DT-A) expression cassette added to the 3' end was used to eliminate clones having landom integration of the targeting vector. The targeting vector for this LPO deletion (Suppl. Fig. 3) was linearized with *Sac*II digestion, then was introduced into C57BL/6 embryonal stem cells by electroporation (200V, 800 μF, Low Ω, CELLPORATOR, LIFE TECHNOLOGIES). The transformed ES cells were cultured and screened in ES Medium containing 150 μg/ml G418, and 331 colonies that survived after 1 week were picked. Genotyping was performed by analyzing genomic DNA by PCR. The PCR primers used for

the ES genotyping were designed in the genomic region outside of the targeting vector and within the neomycin resistance gene. As a result of primary selection of homologous recombinants by PCR genotyping, nine ES cells (#95, 139, 169, 173, 194, 336, 372, 376, 380) were obtained. These nine ES cells were further analyzed by Southern blotting. Two clones showing evidence for homologous recombination, #169 and 173, were injected into Balb/c blastocysts using standard techniques. Healthy injectioned blastocysts were transferred to the pseudopregnant ICR female recipients to obtain chimeric mice. The obtained chimeric male (designated 173-1), having more than 50% coat color contribution, was mated to C57BL/6 females for germline transmission. The F1 mice thus obtained were genotyped by PCR to confirm germline transmission. Heterozygous mice were then interbred to produce homozygous mice.

2.15. Southern blot analysis for LPO ko

Genomic DNA was digested with *Sac* I or *Bcl* I, electrophoresed on an agarose gel, then blotted onto a nylon membrane (VacuGene XL, GE Healthcare). For 5′ probe, a 349 bp DNA fragment was PCR-amplified using forward primer (5′-ATGAAGCTTTCTCGTCTGTACTGTT-3′) and reverse primer (5′-AATACAACTTAACCCCTCAGCTCTC-3′). For the 3′ probe, a 297 bp DNA fragment was PCR-amplified using forward primer (5′-GATTGTTTGAGTTGGAAATAGCAGT-3′) and reverse primer (5′-GATGCAAGATGTCTGGCTCTAATA-3′). Hybridization and signal detection was performed using an AlkPhos Direct Labeling Reagent (GE Healthcare) in accordance with the manufacturer's instructions. Expected DNA fragments of wild-type and mutant alleles after digestion of genomic DNA with *Sac* I and *Bcl* I were hybridized with probes 5′ probe and 3′ probe, respectively.

2.16. Collection of milk from mice

The milking procedure of Kawakami et al. [39] was followed. The dam and her litter were separated for approximately 2 h prior to milking. Oxytocin (O3251, Sigma Chemical Co.) was administered by hypodermic injection at 0.1 ml (1 IU), 10 min prior to the start of milking. Anesthesia was maintained with 2.0% halothane with a face mask with room air. A one-handed milking device (KN-591, Natsume Seisakusho Co. Ltd., Tokyo, Japan) was employed for milk collection. Milk was stored on ice and immediately assayed XOR activity.

2.17. Bacterial growth experiment

The commercially available *Escherichia coli* strain JM109 was used in the experiment monitoring bacterial growth. Single colonies of JM109 cells were incubated overnight in Luria-Bertani (LB) liquid medium at 37 °C and 250 rpm. The overnight culture was diluted 100-fold with freshly prepared LB liquid medium, and pre-cultured for 2h at 37 °C and 250 rpm. Twenty μl of pre-cultured *E. coli* was then used to inoculate 20 ml of LB or M9 minimal medium containing test materials and incubated at 37 °C and 250 rpm. The optical density at 600 nm was measured hourly to monitor bacterial growth.

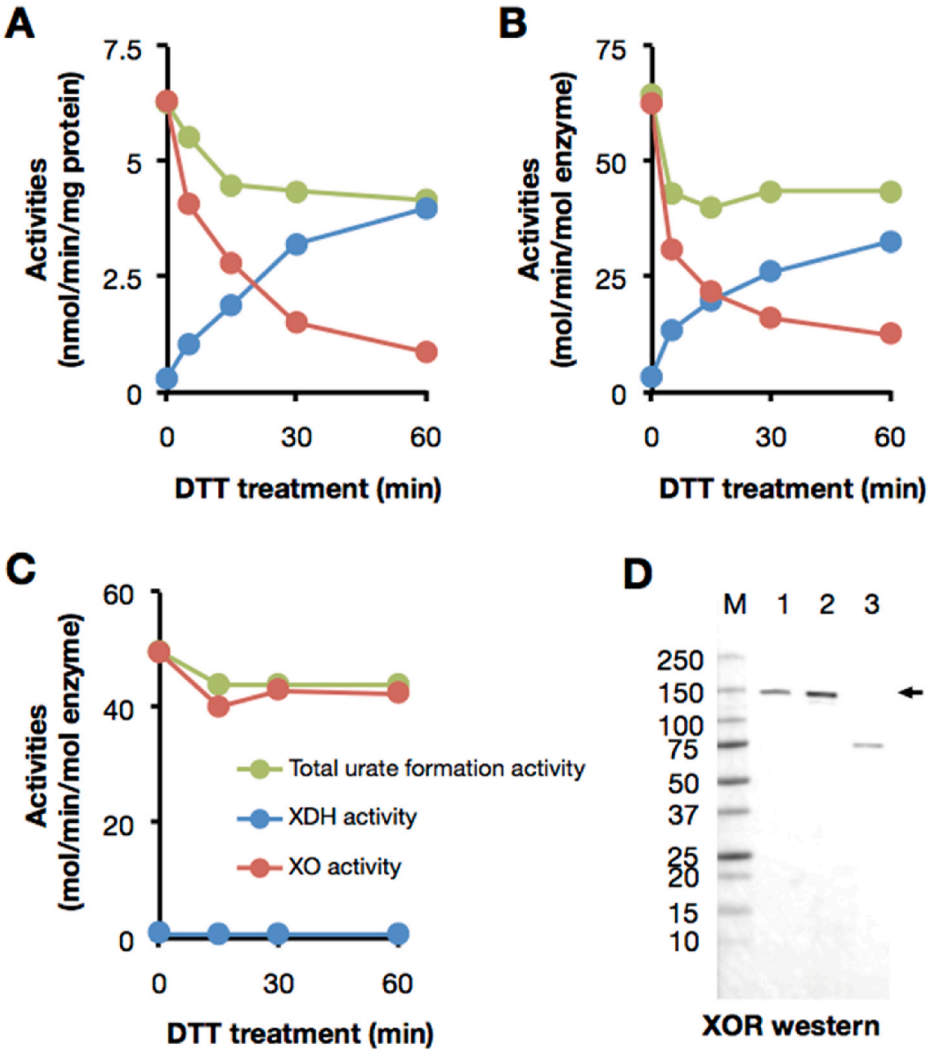

Fig. 1. Bovine milk XOR used in this experiment is re-convertible to XDH with thiol reducing agent. (A–C) XOR samples were treated with 10 mM DTT at 25 °C. Reactants were withdrawn after incubation at the time interval indicated in figures and XOR activity was measured by the method described in the *Materials and methods*. (A) Endogenous XOR in whole milk, (B) Purified XOR from bovine milk (2 μM) used in the present experiments, (C) A commercially obtained XO sample (2 μM). The activities were indicated as follows; NAD^+ plus O_2-dependent urate formation (green: total urate formation activity), O_2-dependent urate formation (red: XO activity), and NAD^+-dependent NADH formation (blue: XDH activity). (D) Western blot analysis was performed in a 5–20% polyacrylamide gel. Lane M, molecular mass standards (Precision Protein Standards, Bio-Rad Laboratories); lane 1, bovine whole milk; lane 2, purified XOR from bovine milk used in the experiments; lane3, commercially available XO from bovine milk. Lane 1 contains 0.8 μg of protein and lane 2 and 3 contain 0.08 pmol of enzyme. XOR (shown as arrow) was detected with anti-rat XOR antibody. (For interpretation of the references to color in this figure legend, the reader is referred to the Web version of this article.)

3. Results

3.1. XDH/XO converting (D→O) activity in milk and analysis of necessary components

Fresh bovine milk normally contains only the oxidase form of xanthine oxidoreductase, but when pure lipase rather than pancreatin (which contains abundant proteases [16].) is used in the purification [25] it can be fully converted back to the initially expressed XDH form by incubation with dithiothreitol (DTT) (Fig. 1A and B). This retro-conversion involves reduction of specific protein disulfides present in the oxidase form back to cysteines [40]. By contrast, commercially available bovine milk XO, whose purification includes pancreatin treatment, cannot be returned to a dehydrogenase form by treatment with a reducing reagent (Fig. 1C) due to limited proteolysis as judged by Western blot analysis (Figs. 1D-3) [16]. We first investigated whether milk retains the ability to convert exogenous XDH to XO (Fig. 2). To exclude any possible effect of endogenous XOR in this experiment, residual XOR was removed from the whey fraction by ultrafiltration using a 100 kDa exclusion membrane (Fig. 2A). No endogenous O_2- or NAD^+-dependent xanthine oxidization activity was observed in the filtrate (Fraction II), indicating that all endogenous XOR had been trapped by the 100 kDa exclusion membrane (data not shown). Fig. 2B illustrates that exogenously added XDH is effectively converted to XO upon incubation with Fraction II, indicating that the D→O activity of interest resides in Fraction II (Fig. 2A). The activity is heat labile, being lost when Fraction II was boiled for 5 min at 95 °C (Fig. 2B). Most of the whey D→O activity is recovered in Fraction II, with only 8% of D→O activity trapped with the 100 kDa exclusion membrane, indicating that SO (which like XDH is retained by the 100 kDa exclusion membrane) is not responsible for the D→O activity present in Fraction II.

Fraction II was further fractionated by ultrafiltration with a 30 kDa exclusion membrane to further assess the size distribution of the D→O activity. As shown in Fig. 2B, neither the >30 kDa fraction (Fraction L) nor the small molecular weight fraction (Fraction S) has significant D→O activity, but D→O activity is recovered upon recombining Fractions L and S, indicating that both fractions contained components necessary for conversion (Fig. 2B). The component in Fraction L contributing to D→O activity is heat-sensitive, whereas that in Fraction S is not (Fig. 2B). These results indicate that D→O activity relies upon a heat-labile, large molecular weight component, in all likelihood a protein having a molecular weight between 30 and 100 kDa, and a heat-stable small molecular weight component; the two do not tightly associate, as reflected in the ease with which they are separated by ultrafiltration.

3.2. Identification of the protein component responsible for D→O activity as LPO

Fraction L was further purified to homogeneity according to the methods as described in Supplementary Fig. S1 (Supplementary material, Section 1). The purified protein showed the same size as authentic bovine milk lactoperoxidase (LPO) (Fig. 3A and B) and possessed peroxidase activity, and its specific activity with the reducing substrate 2,2′-azino-bis (3-ethylbenzothiazoline-6-sulfonic acid) (ABTS) was 1670 mmol min^{-1} (mg protein)$^{-1}$. On SDS-PAGE analysis, it was found that the putative protein factor could be LPO. Further N-terminal amino acid sequence of the protein factor was performed by automated Edman degradation on a PVDF-membrane. The resulting amino acid sequence is DTTLT-VTD, identical to the N-terminal amino acid sequence of the mature form of bovine LPO [41]. The UV–visible absorption spectrum of the purified protein factor exhibited the characteristic absorption peak of LPO at 412 nm (Fig. 3C) and was indistinguishable from the absorption spectrum of the authentic peroxidase (Fig. 3C). Thus, the protein component responsible for D→O activity in milk is established to be LPO.

3.3. Catalytic properties of LPO relevant to D→O activity

O_2-dependent urate formation (XO activity) and NAD^+-dependent NADH formation (XDH activity) does not change during the incubation of purified XDH with LPO alone, indicating that LPO alone did not convert XDH to XO (Fig. 4A). However, as shown in Fig. 4B, XDH is efficiently converted to XO when an aliquot of Fraction S was added to the D→O assay. In addition, the D→O activity accelerates significantly by the addition of hydrogen peroxide (H_2O_2) (Fig. 4C). A close comparison indicates that there is no difference between the D→O activity of the purified protein factor of D→O/Fraction S/H_2O_2 system and that of purified LPO/Fraction S/H_2O_2 (data not shown). Cyanide forms an inhibitory complex with peroxidases [42,43], and we find that the D→O activity of LPO/Fraction S/H_2O_2 is strongly inhibited with 0.5 mM of potassium cyanide (Fig. 4D). These results are all consistent with the

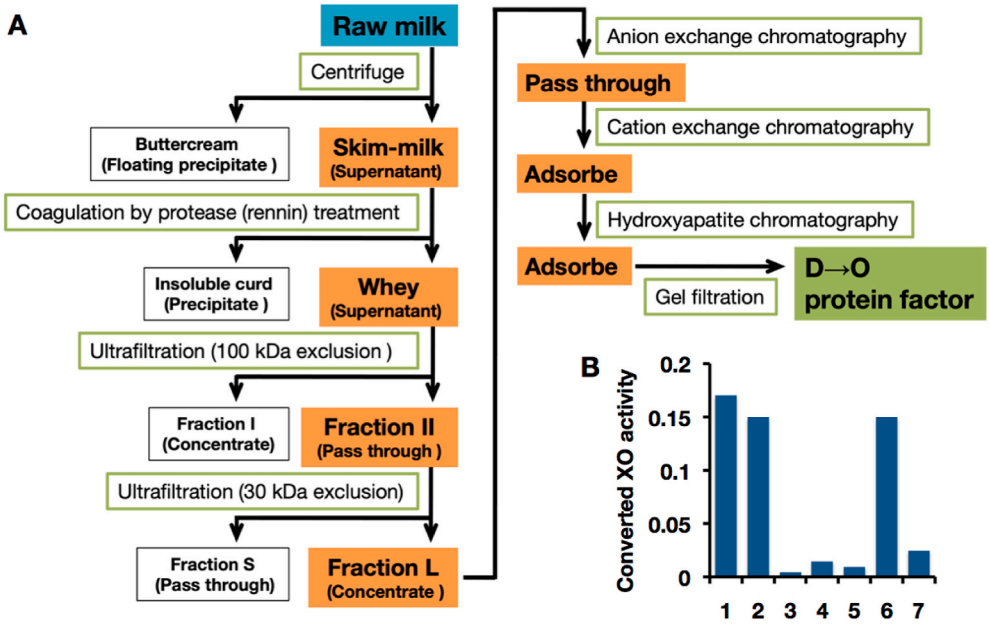

Fig. 2. Purification and characterization of the *D→O* protein factor in Fraction L. (A) The steps of purification strategy starting with bovine milk are depicted as a flow-chart. Fractions containing D→O activity are shaded in orange. Detailed conditions and chromatograms for anion exchange, cation exchange, and hydroxyapatite were described in SupplementaryFigure S1 (Supplementary material, Section 1). Result of gel filtration chromatography was indicated in Fig. 3A. (B) Characterization of bovine milk D→O activity. Exogenous purified XDH was incubated with the bovine milk Fractions. 1, Fraction II; 2, mixture of Fractions L and S; 3, Fraction L; 4, Fraction S; 5, heat denatured Fraction II; 6, mixture of Fraction L and heat denatured Fraction S; 7, mixture of heat denatured Fraction L and Fraction S. Converted XO activity was indicated as O_2-dependent urate formation (nmol/min). (For interpretation of the references to color in this figure legend, the reader is referred to the Web version of this article.)

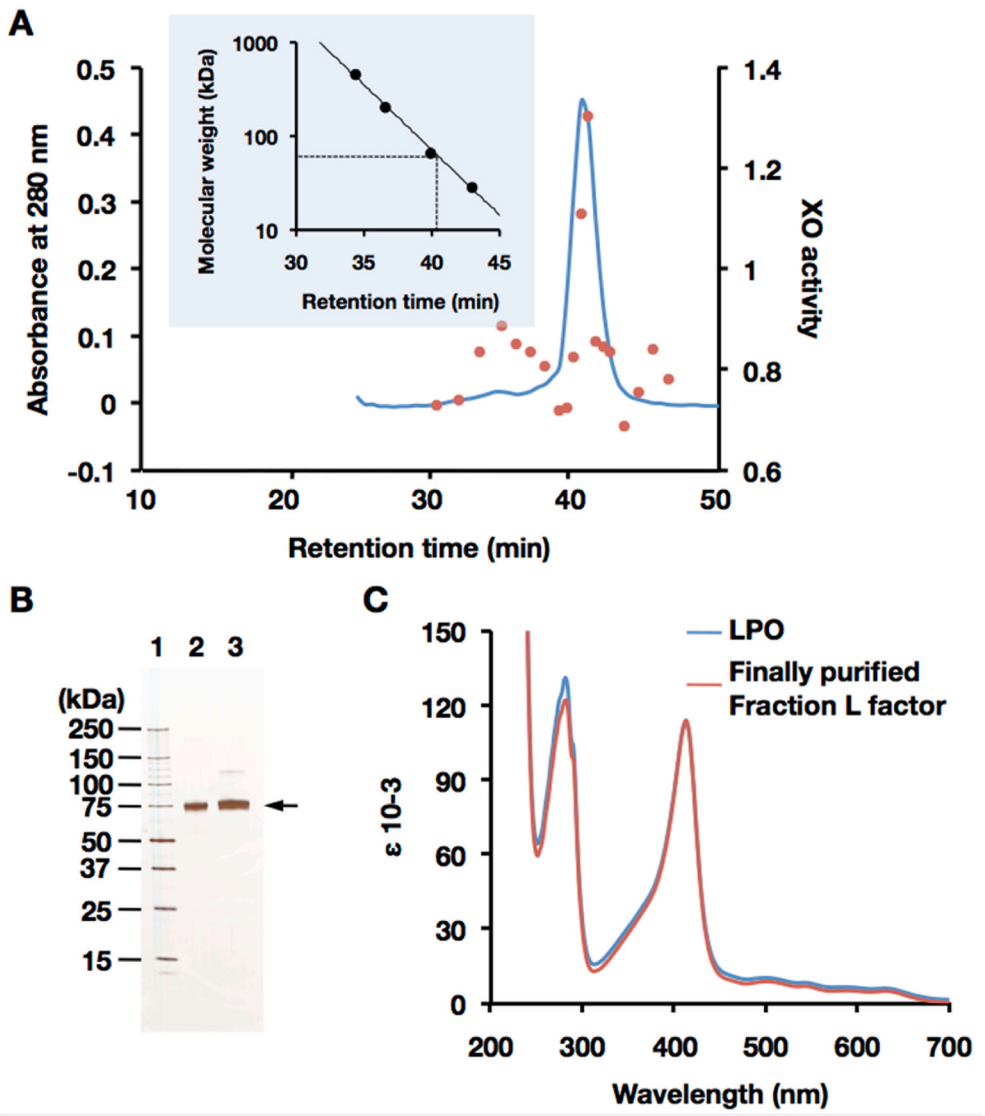

Fig. 3. Identification of the *D→O* protein factor. (A) Purification of the *D→O* protein factor from Fraction L by gel filtration chromatography on Superose 6. Proteins were eluted with 200 mM sodium chloride in 50 mM sodium phosphate buffer, pH7. D→O activity of each fraction was measured and demonstrated the same method as described in Supplementary material Section 1. Blue line, absorbance at 280 nm; red circle, relative XO activity. XO activity was represented in O_2-dependent urate formation (nmol/min). *Insert*: a standard curve for molecular weight estimation. (B) SDS-PAGE analysis of the protein factor of D→O system isolated from bovine milk. Analysis was performed in a 5–20% polyacrylamide gel. Lane 1, molecular mass standards (Precision Protein Standards, Bio-Rad Laboratories); lane 2, commercially available LPO from bovine milk; lane 3, purified D→O protein factor (shown as arrow) from Fraction L. Each lane contains 200 ng of protein. The gel was silver-stained. (C) UV–visible absorption spectrum of the purified D→O protein factor from bovine milk (red line). Commercially available LPO from bovine milk (blue line) was used as a comparison. $\varepsilon = \log_{10}(I_0/I)/c.l)$. c = molar concentration of enzyme, l = optical light path in cm. (For interpretation of the references to color in this figure legend, the reader is referred to the Web version of this article.)

conclusion that peroxidase is necessary but not sufficient for the D→O activity. To whether D→O activity is specific to LPO, horseradish peroxidase (HRP) has been assayed for D→O activity in the presence of H_2O_2, as shown in Fig. 5B, and is found to be unable to convert XDH to XO under these reaction conditions. We conclude that D→O activity is specific to LPO.

3.4. *Identification of the small molecular weight component of D→O activity*

SCN^- is a natural component of milk [44], and we have found that Fraction S contains 40–100 μM of SCN^- as determined calorimetrically using ferric nitrate [37]. The retention volume of SCN^- and D→O activity are identical when Fraction S is subjected to gel filtration chromatography (Supplementary material, Section 2, Fig. S2). We have also tested whether SCN^- can substitute for Fraction S in the D→O assay and find that indeed it is effective in converting XDH to XO (Fig. 5A). In contrast, SCN^- is not effective when HRP rather than LPO is used in the assay (Fig. 5B). This result is consistent with the observation that HRP oxidizes SCN^- one hundredfold more slowly LPO at optimum pH [45]. Finally, treatment of Fraction S with thiocyanate hydrolase (SCNase) is found to significantly diminish D→O activity (Fig. 5C). We thus conclude that thiocyanate is the low molecular weight component responsible for D→O activity in milk, and that just the three components LPO, SCN^- and H_2O_2 are necessary and sufficient for conversion of XDH to XO in milk.

3.5. *Characterization of D→O activity in a fully defined LPO/SCN^-/H_2O_2 system*

The XO that was formed by D→O conversion was reconverted reversibly to XDH upon incubation with 10 mM dithiothreitol (DTT) for about 30 min, indicating that oxidation of cysteine residues to give one or more disulfide bonds is involved in the conversion process (Figs. 4C and 5D). To identify the specific cysteines involved, three variants of rat XOR in which specific cysteine residues known to be required for D→O conversion [26] were incubated in turn with the reconstituted D→O conversion system and D→O activity assessed (see responsible cysteine residues conversion from XDH to XO Fig. 6A, Cys^{535}, Cys^{992}, Cys^{1316}, and Cys^{1324}). Native XDH from rat liver was converted to XO similarly to the bovine enzyme: more than 95% of XDH was converted to XO within 20 min by the reaction with the reconstituted D→O system (Fig. 5D). Total activity also increase concomitant with D→O because the turnover number of XO was higher than that of XDH. On the other hand, only incomplete conversion was observed when the experiment was repeated with variants of the rat enzyme in which Cys ^{535} and Cys^{992} were

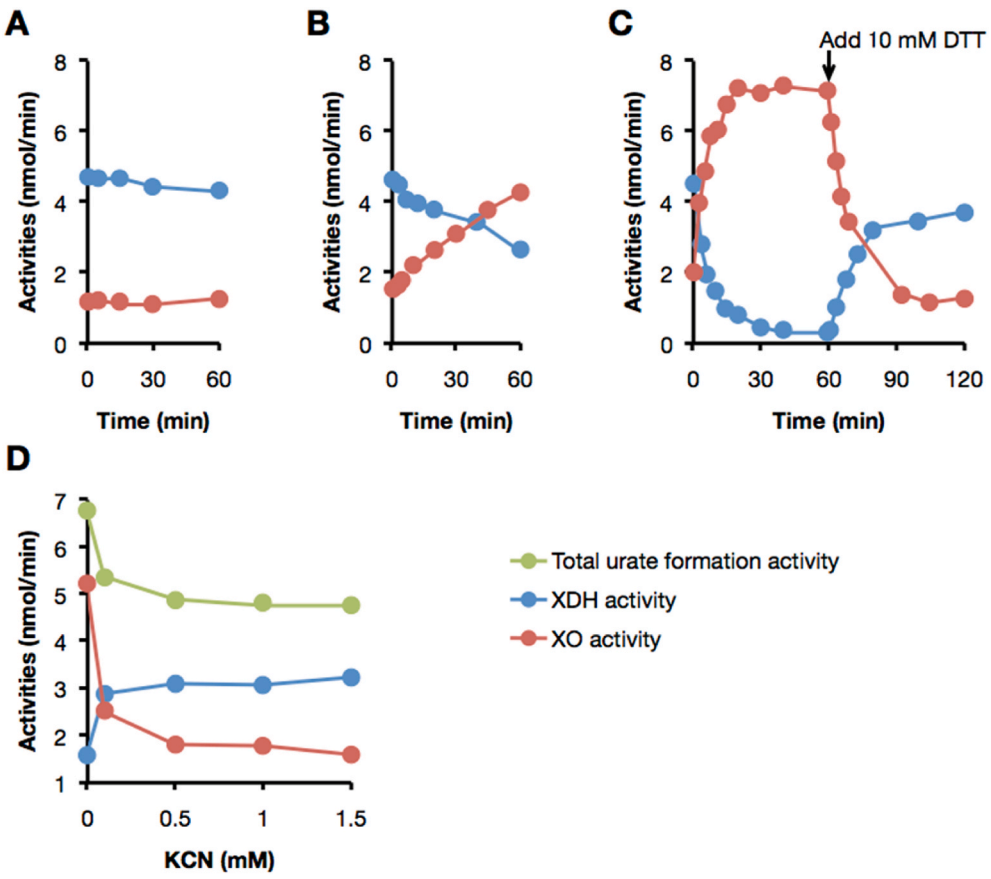

Fig. 4. Characterization of *D→O* reaction mediated by lactoperoxidase. The experimental procedures and conditions are the same as in Fig. 2 other than LPO and H_2O_2 were used instead of milk fraction. Aliquots were withdrawn at the indicated intervals and XOR activity was determined. O_2-dependent urate formation (red circles: XO activity); NAD^+-dependent NADH formation (blue circles: XDH activity); NAD^+ *plus* O_2-dependent urate formation (green circles: total urate formation activity). (A) The D→O assay with LPO, (B) LPO and Fraction S and (C) H_2O_2. The arrow shows the time at which DTT (10 mM, final concentration) was added to reaction mixture. (D) Inhibition of LPO-mediated D→O reaction by potassium cyanide. After XDH was incubated with LPO, Fraction S, and H_2O_2 in the presence of 0, 0.1, 0.5, 1.0, 1.5 mM of potassium cyanide for 20 min, the D→O activities are examined. It was known that both XDH and XO can be inactivated by cyanide only in oxidized form, but it was not in reducing form and therefore during enzyme reaction inactivation is minimum [69]. The experiments are performed in the presence of substrate therefor effect of cyanide on XOR activities are limited. On the other hand, Peroxidase is a heme protein that is known to be completely inhibited by cyanide [42]. (For interpretation of the references to color in this figure legend, the reader is referred to the Web version of this article.)

mutated to other amino acids (Fig. 5E). Furthermore, two other mutants, C535A/C992R/C1316S and C535A/C992R/C1324S, were completely resistant to conversion to the oxidase form (Fig. 5F and G). These results are fully consistent with previous results that formation of two specific disulfide bridges – between Cys^{535} and Cys^{992}, and between Cys^{1316} and Cys^{1324} – are responsible for conversion of XDH to XO (Fig. 6A).

3.6. The conversion of XDH to XO in bovine milk

On the basis of the above, the mechanism by which XDH is converted to XO in bovine milk can be summarized as shown in Fig. 6A. H_2O_2 generated by the reaction of O_2 with either XDH [9,21,46] (also see Fig. 6C) or XO reacts with endogenous SCN^- to generate hypothiocyanite ($OSCN^-$). In the presence of LPO, this induces disulfide formation in XDH, resulting in its conversion to XO. The process is autocatalytic in the sense that as XDH is converted to XO, progressively more H_2O_2 is generated. This is illustrated in Fig. 6B, where the O_2 -dependent formation of urate seen upon incubating XDH with LPO, SCN^- and xanthine, exhibits a pronounced lag over the first ~200 s. As XDH is converted to XO, urate formation increases, reaching a maximal rate after ~600 s that is considerably faster than the rate of urate production seen in the absence of LPO and SCN^- (Fig. 6B). Virtually identical results are obtained when bovine milk Fraction II is used instead of the reconstituted D→O system (Fig. 6B). D→O conversion was inhibited with XOR inhibitor (Supplementary Fig. S3), because the conversion reaction was proceeded with XO activity.

We next analyzed bovine milk for purines to determine whether they might serve as reducing substrates for the D→O activity seen in our model. We determined the purine levels in fresh milk (after addition of salicylate and immediate freezing, with and purines levels subsequently determined within ~8 h). In one cow, the xanthine concentration was found to be 5.76 ± 0.13 μM and urate 81.5 ± 7.2 μM; xanthine and urate levels of 4.65 ± 0.28 μM and 118.5 ± 27.9 μM, respectively in milk from another cow, suggesting that sufficient amounts of xanthine are indeed initially present immediately after lactation to provide the reducing power to reduce O_2 to H_2O_2 in milk and contribute to the observed D→O conversion.

3.7. Effect of free sulfhydryl group on reconstituted milk D→O system

Hypothiocyanite is a major oxidant generated by LPO and it react specifically with sulfhydryl groups in biological molecules [47]. Glutathione (GSH) contains free sulfhydryl group and effective substrate for hypothiocyanite [47,48]. D→O was initiated by the inner molecular disulfide formation, and hypothiocyanite was involved in the sulfhydryl oxidation in the milk system.

Fig. 7 shows the effect of GSH on the reconstituted milk D→O system. Free sulfhydryl group competes disulfide formation in XOR molecule, GSH completely interrupt D→O reaction (Fig. 7A).

Sulfhydryl oxidation by reconstituted milk D→O system was evaluated. No sulfhydryl was detected in the group which was provided GSH as an extrinsic sulfhydryl to the reconstituted milk D→O system (Fig. 7B, Control). Almost all the extrinsic sulfhydryl was oxidized by D→O system. The sulfhydryl oxidation reaction was initiated with the XO activity (Fig. 6A and C), therefore XOR inhibitor, allopurinol, topiroxostat, and febuxostat, effectively inhibited extrinsic sulfhydryl oxidation (Fig. 7B).

3.8. Generation of LPO knock-out mouse

To confirm the physiological involvement of LPO in the D→O conversion *in vivo*, we constructed a mouse knockout line that was deficient the *Lpo* gene (Supplementary material, Section 4, Fig. S4). Correct homologous recombination was confirmed by Southern blot analysis (Supplementary material, Section 5, Fig. S5). The results indicate that

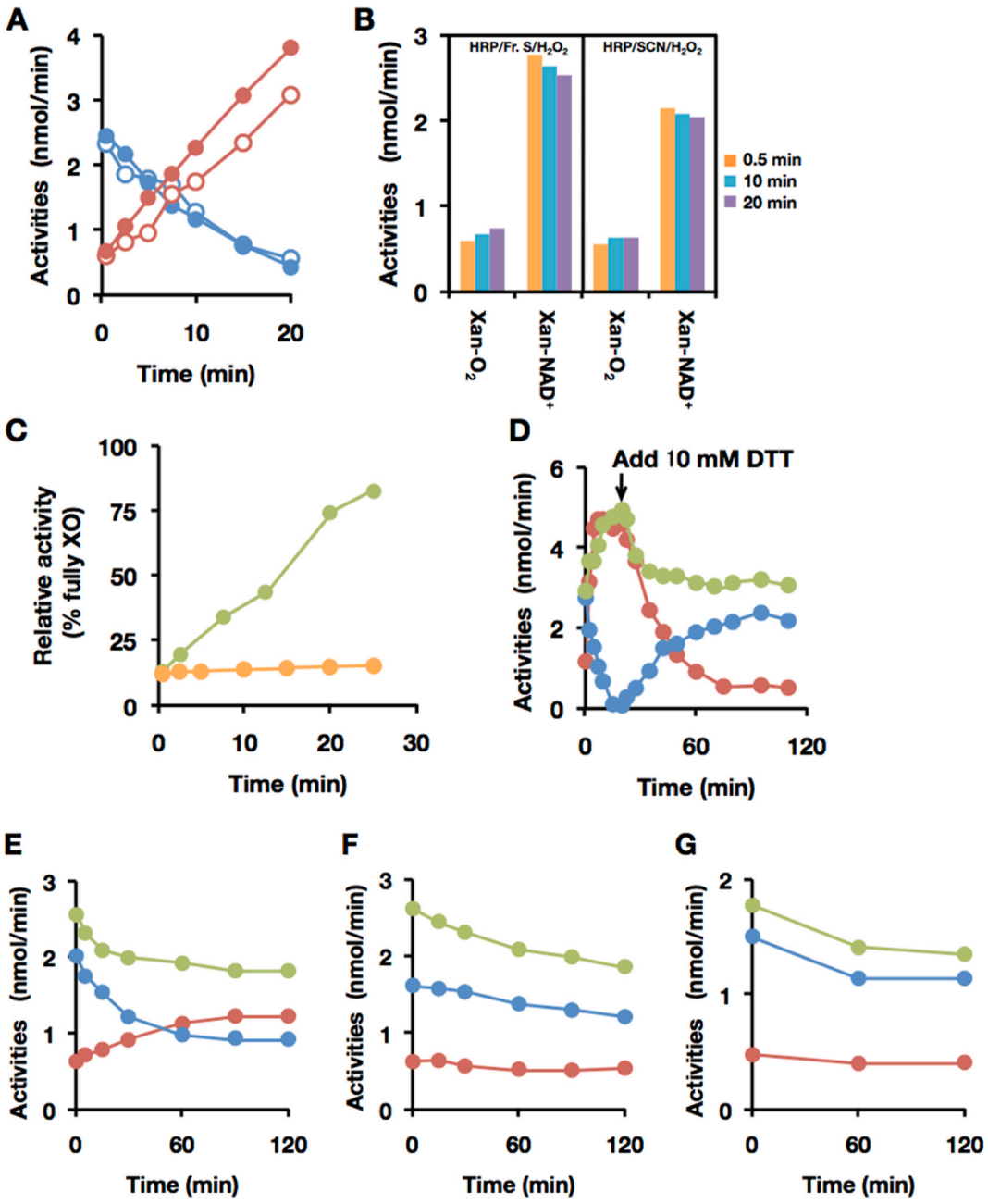

Fig. 5. Characterization of the *D→O* factor in Fraction S. (A–C) Effect of thiocyanate on peroxidase-catalyzed D→O activity, using LPO and HRP. The experimental procedures and conditions are the same as described in Fig. 2 other than LPO, HRP and NaSCN were used instead of milk fraction. (A) D→O reaction with LPO/Fraction S/H_2O_2 (filled circles), or LPO/SCN^-/H_2O_2 (open circles). Red circles, O_2-dependent urate formation for XO activity; blue circles, NAD^+-dependent NADH formation for XDH activity. (B) D→O reaction with HRP/Fraction S/H_2O_2 (left panel), or HRP/SCN^-/H_2O_2 (right panel). O_2-dependent urate formation for XO activity (Xan-O_2) and NAD^+-dependent NADH formation for XDH activity (Xan-NAD^+) were assayed at indicated time. (C) Effect of SCNase treatment of Fraction S on D→O activity. Bovine milk XDH was incubated with LPO/Fraction S/H_2O_2 (green circles), or LPO/SCNase treated Fraction S/H_2O_2 (orange circles). (D–G) LPO-catalyzed D→O of rat XOR variants. The experimental procedures and conditions are the same as described above except for the rat XOR variants. Red circles: O_2-dependent urate formation, blue circles: NAD^+-dependent NADH formation, and green circles: NAD^+ *plus* O_2-dependent urate formation. (D) 2 μM native-XDH (from rat liver, AFR 146, D/O 8.06), (E) 1 μM Rat liver XDH C535A/C992R mutant (AFR 129, D/O 7.42), (F) 1 μM Rat liver XDH C535A/C992R/C1316S mutant (AFR 106.4, D/O 5.06), or (G) 0.5 μM Rat liver XDH C535A/C992R/C1324S mutant (AFR 98.7, D/O 9.125), were incubated with LPO/NaSCN/H_2O_2. The arrow shows the time at which DTT (10 mM, final) was added in experiment *D*. (For interpretation of the references to color in this figure legend, the reader is referred to the Web version of this article.)

the targeted allele is transmitted into the germline, and non-specific insertion of targeting vector into the mouse genome has not occurred (Fig. S5). Loss of LPO in LPO-ko mice has been confirmed by Western blot analysis of a milk sample, using anti-mouse LPO antibody (Fig. 8A). Growth of LPO-ko mice with body weight gain, and the estimation of survival distribution using the Kaplan-Meier method were no noticeable difference between LPO-ko mice and their WT littermates (Fig. S6).

3.9. Milk XO content in LPO knock-out mice

It is well known that lactation is largely dependent on hormonal state and condition [49]. XOR activity in mouse milk samples, obtained

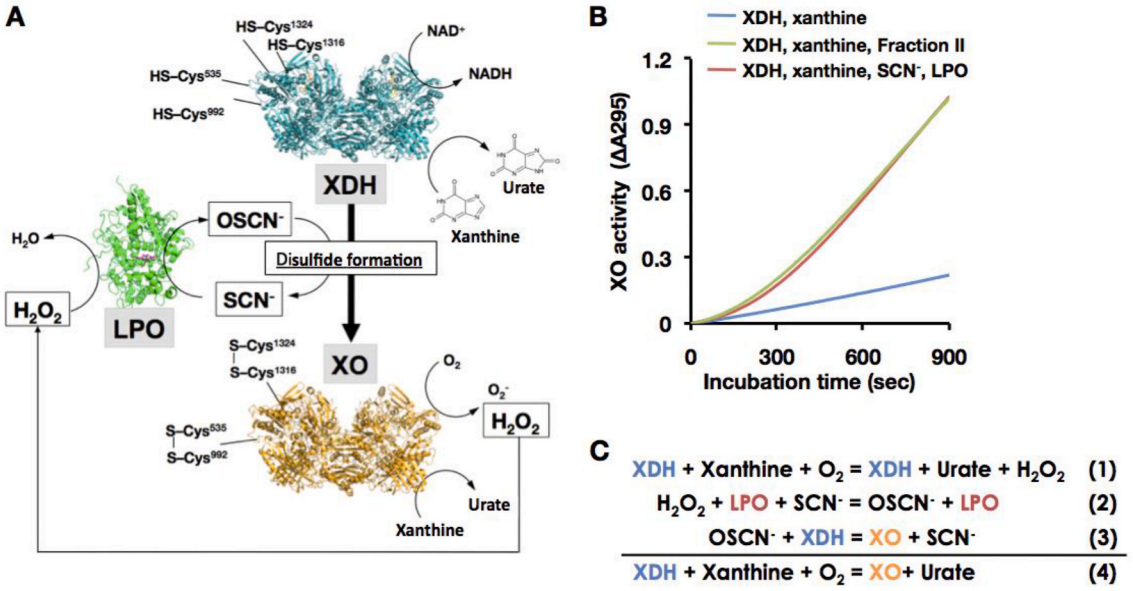

Fig. 6. Physiological involvement of LPO/SCN/H_2O_2 system to the *D→O* reaction. (A) The Illustration for D→O activity in bovine milk. Enzyme structures are designed from bovine lactoperoxidase (LPO, PDB ID: 3NYH) [70] and rat xanthine oxidase (XO, PDB ID: 4YTZ) [12], and rat XOR C535A, C992R, and C1324S triple valiants (XDH, PDB ID: 1WYG) [26] are used here. Those corresponding residues are all conserved within mammalian XOR. Cysteine residues (Cys535, Cys992, Cys1316, and Cys1324) responsible for disulfide bridge formation were depicted on the protein structures. When a part of XDH is converted to XO, H_2O_2 is generated from XO in the presence of xanthine. The generated H_2O_2 will then participate in the LPO/H_2O_2/SCN^- reaction, resulting in disulfide bond formation and conversion of the dehydrogenase to the oxidase. D→O may well be accelerated synergistically/autocatalytically, also *in vivo*. (B) Synergistic D→O. Reaction was carried out in the mixture containing 0.1 M pyrophosphate buffer pH8.5, 0.2 mM EDTA, 150 μM xanthine, and116 units/ml SOD (blue line), with additional 50 μM NaSCN plus 1 nM LPO (red line) or 10% bovine milk Fraction II (green line) at 25 °C. The reaction was started by addition of 20 nM XDH to the mixture. The increase in XO activity was monitored by the optical absorbance at 295 nm as O_2-dependent urate formation. (C) Reaction mechanism for synergistic D→O. (For interpretation of the references to color in this figure legend, the reader is referred to the Web version of this article.)

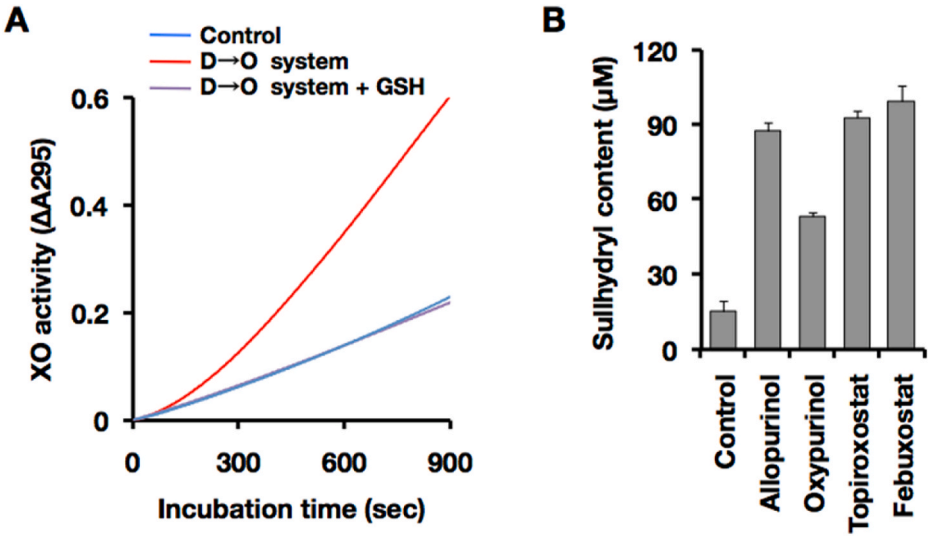

Fig. 7. Effect of free sulfhydryl group or XOR inhibitor on the milk *D→O* system. (A) Inhibition of synergistic D→O with free sulfhydryl group. Reaction was carried out in the same condition of Fig. 6B (blue line, XDH control; red line, complete D→O system) except for addition of GSH in the reaction (magenta line, complete D→O system + GSH). (B) *D*, Oxidation of free sulfhydryl group by milk D→O system. Milk D→O system was reconstituted with 20 nM XOR, 1 nM LPO, 150 μM xanthine, and 50 μM SCN^-. Reduced glutathione (GSH, 100 μM) was co-incubated with reconstituted milk D→O system presence or absence of the XOR inhibitor in 0.1 M pyrophosphate buffer (pH 8.5) and 0.2 mM EDTA for 20 min at 25 °C. Residual sulfhydryl group was determined with DTNB by the method described in the *Materials and methods*. Concentrations of each XOR inhibitor are as follows: allopurinol, 10 μM; oxypurinol, 10 μM; topiroxostat, 1 μM; and febuxostat, 1 μM. Control, without XOR inhibitor. Results are expressed as the mean ± SD (n = 5 per group). (For interpretation of the references to color in this figure legend, the reader is referred to the Web version of this article.)

immediately after hormonal treatments, was next assessed as described in Experimental procedures. While almost all the milk XOR activity is present as XO in wild-type mice, almost 60% was present as XDH in the milk from a knock-in (XDH-ki) mouse mutant encoding an XDH (C995R) that could not be converted to XO (Fig. 8B). This partial loss of D→O activity can be explained by another couple of cysteine residues (Cys1316-Cys1324) being involved in the conversion [12,26] and also XO activity of the XDH form itself [9,10]. In LPO deficient mice, conversion to XO was also incomplete, with ~40% remaining as XDH in their milk (Fig. 8B). Although XDH in liver lysate was readily converted to XO (Fig. 9A and B), XDH in LPO-ko mouse milk was stable even after incubation at 25 °C (Fig. 9C). Residual XDH in LPO-ko milk was fully converted to XO in the presence of exogenously added LPO (Fig. 9C). These indicate, however, that LPO is indeed involved in the milk D→O reaction.

It is important to recognize that LPO and XDH are expressed in different cells types of the mammary gland [5], and come together only in the course of lactation [50]. Even so, it is to be noted that LPO

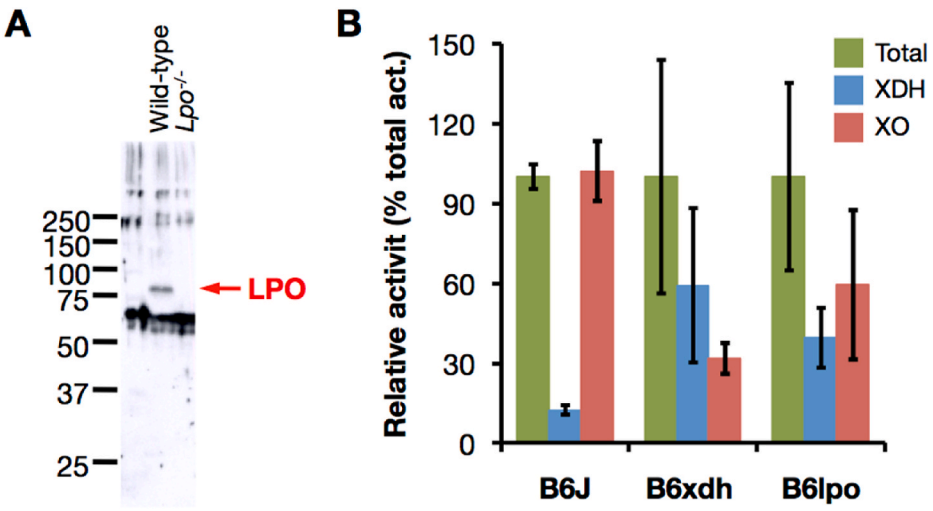

Fig. 8. Characterization of LPO knock-out mouse. Deficiency of LPO in LPO-ko mouse was confirmed by the analysis of milk. (A) Western blot analysis of the mice milk. Lane Wild-type, whole milk from wild-type mouse; lane $Lpo^{-/-}$, whole milk from LPO-ko mouse. An anti-mouse LPO antibody, which cross-reacts with LPO protein in milk fraction from wild-type counterpart (shown as arrow), cannot detect LPO from LPO-ko milk. Each lane contains 5 μg protein. Molecular mass standards (Precision Protein Standards, Bio-Rad Laboratories) (B) Milk XOR activity was compared in wild-type (B6J, n = 3), XDH-stable mutant (B6xdh, n = 3), and LPO-ko (B6lpo, n = 5), mice. XOR activity was measured by the method described in the *Materials and methods* immediately after milking. Bar graphs show mean ± SD. The total (NAD^+ *plus* O_2-dependent) urate formation (green bar), O_2-dependent urate formation (red bar: XO activity), and NAD^+-dependent NADH formation (blue bar: XDH activity) were indicated as a percentage value of the total urate formation activity. (For interpretation of the references to color in this figure legend, the reader is referred to the Web version of this article.)

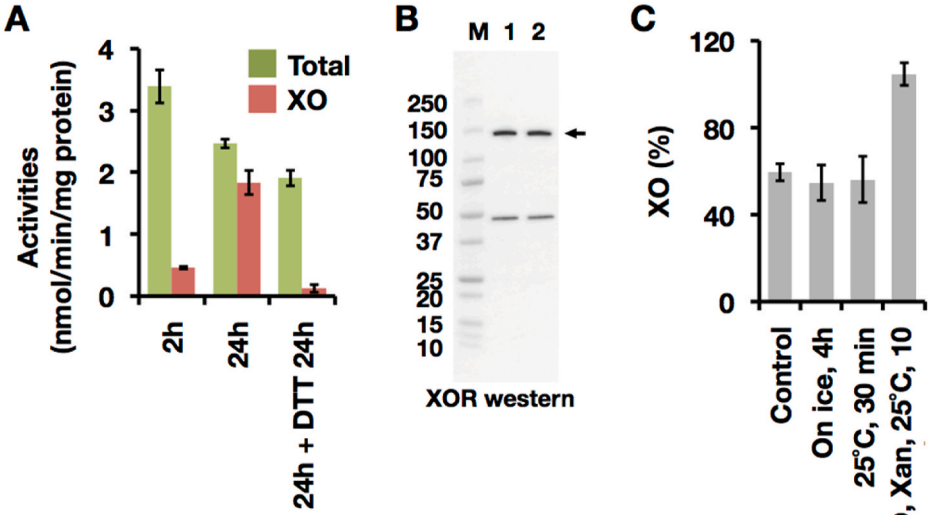

Fig. 9. Spontaneous conversion of XOR activity in mouse liver lysate and LPO knock-out mouse milk by disulfide bond formation. Gently prepared liver lysate was added to the XOR assay reaction medium with 3% of final concentration and assayed as described in the *Materials and methods*. (A) XOR activity of liver lysate was assayed within 2h from the start of tissue homogenization (2h), after 24 h on ice stock (24h), or treated with 10 mM DTT for 24 h after 24 h on ice stock. The total (NAD^+ plus O_2-dependent) urate formation (green) and O_2-dependent urate formation (red: XO activity). Results are expressed as the mean ± SD (n = 5 per group). (B) XOR (shown as arrow) was detected with anti-rat XOR antibody. Lane 1, liver lysate within 2h from the start of tissue homogenization; lane 2, after 24 h on ice stock. Each lane contains 10 μg of protein. (C) LPO-ko mice milk were assayed to evaluate the stability of endogenous XDH activity. XOR activity was assayed as described in *Materials and Methods* immediately after milk preparation (Control), incubated for 30 min at 25 °C (25 °C, 30 min), or stand on ice 4 h (On ice, 4h). The activities were indicated as XO content which was indicated by the percentage of O_2-dependent urate formation to total (NAD^+ plus O_2-dependent) urate formation. Residual XDH activity was converted by addition of LPO and xanthine (LPO, Xan, 25 °C, 10 min). Results are expressed as the mean ± SD (n = 3 per group). (For interpretation of the references to color in this figure legend, the reader is referred to the Web version of this article.)

deficient mice still manifest a significant amount of XO activity (40–60%), suggesting that in addition to XO activity of XDH itself as shown in Fig. 1, SO may also be involved to some extent in the observed D→O activity. This will be discussed more in Discussion section.

3.10. D→O activity in lung and salivary gland

XOR is expressed as XDH in normal tissues, and XO activity content is less than 10% in the immediately prepared supernatant from liver homogenate (Fig. 10A and B). On the other hand, the XO content is almost 30% in the mammary gland where XOR and LPO coexist and they could catalyze the D→O conversion (Fig. 10A and B).

XOR and LPO coexist in organs such as the lung and salivary gland (Supplementary Fig. S7). To confirm this, we have examined the XOR activities in various organs (Fig. 10A and B), and also determined XOR and LPO proteins expressed in salivary gland by Western blot analyses that showed 150 kDa as XOR and 70 kDa as LPO (Fig. 10C and D), consistent with previous reports [22]. Co-expression of LPO and XOR in the salivary gland is thus confirmed. These two enzymes function as a D→O conversion system in salivary gland of WRT mice, as reflected in the fact that the XO content from immediately prepared tissue supernatant, was more than 70% (Fig. 10A and B); the XO level decreased to 30% in salivary glands from LPO-KO mice (Fig. 10A and B).

XO content in the immediately prepared supernatant from lung homogenate was similar level of the mammary gland (Fig. 10A and B). D→O system should be work in lung because XO content was reduced in LPO-KO counterpart (Fig. 10A and B), although LPO could not detect in the lung western analysis.

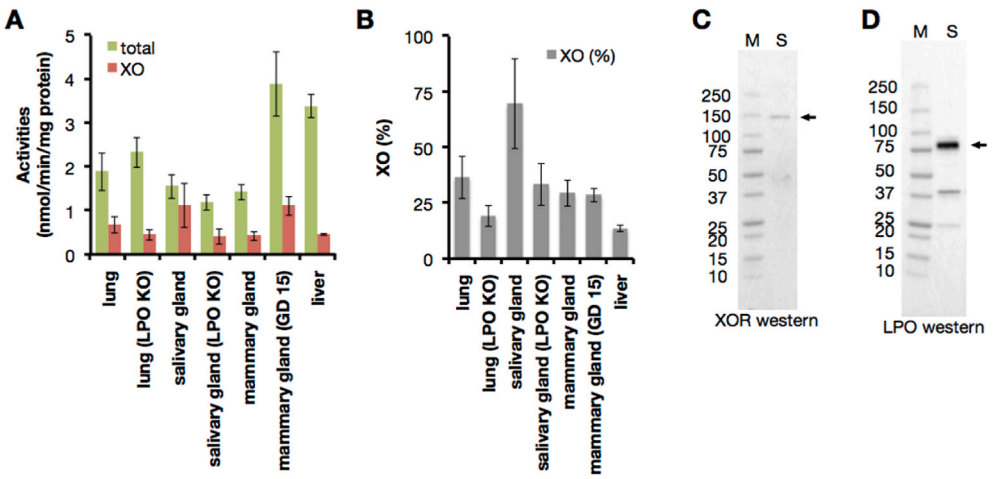

Fig. 10. LPO co-localization with XOR. (A–B) XOR activity of gently prepared tissue lysate were assayed within 2h from the start of tissue homogenization. XOR activity was assayed as described in Fig. 9. LPO KO; LPO knock out mouse, GD; gestational day. Results are expressed as the mean ± SD (n = 5 per group). (A) The total (NAD $^+$ plus O_2-dependent) urate formation (green) and O_2-dependent urate formation (red: XO activity). (B) XO content was indicated by the percentage of O_2-dependent urate formation to total urate formation. (C–D) Western blot analysis was performed in a 5–20% polyacrylamide gel. Lane M, molecular mass standards (Precision Protein Standards, Bio-Rad Laboratories); lane S, salivary gland. Each lane contains 10 μg of protein. (C) XOR (shown as arrow) was detected with anti-rat XOR antibody. (D) LPO (shown as arrow) was detected with anti-mouse LPO antibody. (For interpretation of the references to color in this figure legend, the reader is referred to the Web version of this article.)

3.11. *Effect on bacterial growth with various components in D→O system*

H_2O_2 produced by XO and $OSCN^-$ produced by LPO have strong bacteriocidal activity. To confirm the bacteriocidal properties of D→O reaction products, we evaluated bacterial growth in the presence LPO, XDH, xanthine, and SCN^-. Fig. 11 shows that the growth of *Escherichia coli* in minimal medium ± LPO/XDH/xanthine/SCN^-. The delay in bacterial growth is significant, several hours when all the D→O components were included (Fig. 11-A-a, B-a). The bacteriocidal effect of the D→O system was confirmed when bacteria was cultivated in Luria-Bertani (LB) medium in the cases of Fig. 11 C-a. Given that XO has a central role for the bacteriocidal effect, XOR inhibitors such as Febuxostat, could cancel this bacteriocidal effect (Fig. 11 C-g).

This result indicates that elevated XO levels significantly retard bacterial growth, and could reduce the risk of developing mastitis and similar infection-related complications during lactation. Our results fully support the previous proposals that XO plays an important bacteriocidal role as part of the innate immune system [18].

4. Discussion

Although the conversion of XDH to XO has been proposed to play a role in lactation, it has been shown that transgenic mice in which wild-type XOR was either knocked out altogether or replaced by a variant XDH that cannot be converted to the oxidase form lactated normally [21]. Nevertheless, the predominance of the oxidase form of the enzyme in milk indicates that there is an intrinsic D→O activity in milk, and here we find that milk is indeed able to convert exogenous bovine XDH to XO. The intrinsic D→O system consists of LPO, SCN^- and XO-generated H_2O_2. XOR and LPO are secreted into milk from different cell types in the mammary gland [50–52], indicating that D→O conversion does not occur until their joint appearance in milk in the course of lactation. Xanthine and hypoxanthine are substrates for XO, and in the present study have been detected in relatively low but physiologically significant levels (~5 μM) in milk. Furthermore, much higher concentrations of uric acid (~100 μM) are found, suggesting that more reduced purines were initially present but had become oxidized by enzyme action during lactation. It is thus not surprising that freshly lactated milk retains D→O activity when incubated with exogenous XDH. LPO is an essential

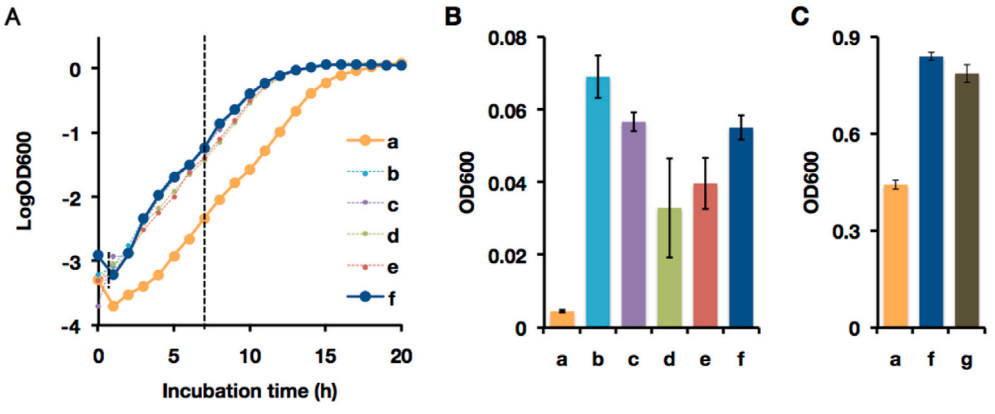

Fig. 11. Effect of a reconstituted milk innate immune system on bacterial growth. (A–C) The bacteriocidal activity of a milk innate immune system consisting of 1 nM LPO, 50 μM NaSCN, 20 nM XDH, and 150 μM xanthine was assessed. To confirm the effect of each component, seven combinations (**a** to **g**) were compared. **a**, Complete system; **b**, without XDH from **a**; **c**, without xanthine from **a**; **d**, without NaSCN from **a**; **e**, without LPO from **a**; **f**, no component; **g**, with 0.1 mM febuxostat to **a**. Heat denatured LPO, NaCl, heat denatured XDH, and urate were used for the negative control of LPO, NaSCN, XDH, and xanthine, respectively. Components of reconstituted milk innate immune system were added to the M9 minimal medium and pre-cultured *E. coli* JM109 was inoculated. Inoculated media were incubated at 37 °C and 250 rpm. To investigate the bacterial growth, the optical density of the culture medium was measured every hour at 600 nm. (A) Representative results for the bacterial growth under each condition. (B) Relative growth on M9 medium after 7 h. The bacterial growth under each condition were compared at the mid-logarithmic growth phase. Results are expressed as the mean ± SD (n = 4 per group). (C) Relative growth on LB medium after 6 h at the mid-logarithmic phase. The concentration of each component was increased from the value described above to 10 nM LPO, 0.5 mM NaSCN, 0.2 μM XDH, and 1.5 mM xanthine. Results are expressed as the mean ± SD (n = 5 per group).

component of a reconstituted D→O system and cannot be replaced by HRP, demonstrating that LPO has a specific physiological role in the D→O conversion as reflected in the results with LPO-knockout mice, which exhibit elevated XDH/XO ratios in their milk as compared to wild-type animals. Still, conversion to XO was not completely suppressed in LPO-knockout mice, indicating a possible contribution of SO which, while not present in milk, may exist in small amounts in various mammary gland cell types in the course of lactation, as shown previously [23,24]. That an SO-dependent D→O activity might be relatively minor is not surprising given the important role SO plays more generally in disulfide formation in the cell, but it may nevertheless be important initiating the autocatalytic D→O conversion identified here. The mammary gland is the defining organ of mammals, and it critically important to protect the mammary gland from bacterial infection such as mastitis for continuous nursing of neonates. Thus, the bacteriocidal activity of D→O activity demonstrated here constitutes another bacterial defense system in addition to the IgA system in mammary gland [53].

The tissue distributions of XOR and LPO do not overlap extensively, although the two enzymes have been reported previously to colocalize in the human salivary gland [54,55], human respiratory mucosa [56] and lung alveolar cells [56,57]. Transcription profiles for LPO (ENSG00000167419.10) and XDH (ENSG00000158125.9) available at The Broad Institute of MIT and Harvard Web site (https://gtexportal.org/home/gene/) by using GTEx Analysis Release V8 (dbGaP Accession phs000424.v8.p2) support these observations [58] (Supplementary Fig. S7), and significant D→O activity is expected in these tissues. The bacteriocidal activity of the milk D→O system demonstrated here is likely functional in these other cell types, and indeed previous work in mice has shown that XO activity increases dramatically in the lung upon infection, likely reflecting conversion of XDH to XO in alveolar cells (although specific enzyme activities and cell type were not determined) [57,59,60].

These specific cell types are known to be prone to SARS-CoV-2 infection, but the D→O conversion system is unlikely to be effective in defending against SARS-CoV-2 infection. It may in fact exacerbate infection through the catalysis of essential disulfide bond formation in the SARS-CoV-2 spike protein. In the three-dimensional structure of SARS-CoV-2, as many as 12–14 disulfide bridges are formed in one of the main subunits of the spike protein [61], which likely improve the stability of the spike protein (Supplementary Fig. S8). Furthermore, although the D→O system likely has no effect on the viral mRNA-dependent polymerase, which does not possess important disulfide bonds [62], its effect on the host's ACE2 receptor may be deleterious. Specifically, a molecular dynamics study has concluded that the binding affinity of the ACE2 receptor for spike protein increases upon disulfide formation in the receptor protein [63]. By facilitating disulfide bond formation in the receptor, thereby raising affinity for virus, it is possible that excess $OSCN^-$ in the salivary gland and lung alveolar cells exacerbates viral infection and facilitates viral propagation by promoting disulfide bond formation in the spike protein of the virus. The above may well explain why SARS-CoV-2 infection is particularly acute in those tissues and cell types that co-express XOR and LPO. Application of the knowledge obtained here to the development of anti-COVID-19 treatment could involve scavenging or inhibition of the formation of the reactive $OSCN^-$ (a key product of the D→O activity involved in disulfide bond formation) in susceptible cell types.

There are a number of reports about the effective therapeutic uses of reduced glutathione [64–66], which might be likely due to scavenging $OSCN^-$. On the other hand, oral administration of XOR inhibitors to prevent $OSCN^-$ formation in gland cells in various diseases is less likely to be beneficial by oral administration of XOR inhibitors. Inhibition of XOR in gout therapy occurs mostly in organ cells such as the liver where the enzyme is abundant and results in increased levels of hypoxanthine in the blood (which can subsequently be incorporated into the cells as IMP and AMP by HGPRT, decreasing *de novo* synthesis of purine nucleotides; [67,68]. Given this situation, it may be difficult for various inflammation diseases to fully inhibit the local formation of $OSCN^-$ in gland cells because the concentration of XOR inhibitor might only incompletely inhibit XO in gland cells. Thus, improved methods to inhibit XOR are needed for effective inhibition of XO where $OSCN^-$ is accumulated.

Funding

This work was supported by JSPS KAKENHI Grant Number JP16205021 & 15H04702 (to Takeshi Nishino).

Declaration of competing interest

There are no conflicts of interest to declare.

Data availability

Data will be made available on request.

Appendix A. Supplementary data

Supplementary data to this article can be found online at https://doi.org/10.1016/j.redox.2022.102573.

References

[1] F.G. Hopkins, Note on the vitamin content of milk, Biochem. J. 14 (6) (1920) 721–724, https://doi.org/10.1042/bj0140721.
[2] E.G. Ball, Xanthine oxidase: purification and properties, J. Biol. Chem. 128 (1) (1939) 51–67, https://doi.org/10.1016/S0021-9258(18)73729-0.
[3] F. Schardinger, Ueber das Verhalten der Kuhmilch gegen Methylenblau und seine Verwendung zur Unterscheidung von ungekochter und gekochter Milch, Z Untersuch Nahrungs Genussmittel 5 (1902) 1113–1121, https://doi.org/10.1007/BF02506750.
[4] M. Dixon, Studies on xanthine oxidase: the specificity of the system, Biochem. J. 20 (4) (1926) 703–718, https://doi.org/10.1042/bj0200703.
[5] E.D. Jarasch, C. Grund, G. Bruder, H.W. Heid, T.W. Keenan, W.W. Franke, Localization of xanthine oxidase in mammary-gland epithelium and capillary endothelium, Cell 25 (1) (1981) 67–82, https://doi.org/10.1016/0092-8674(81)90232-4.
[6] E. Della Corte, F. Stirpe, The regulation of xanthine oxidase in rat liver: Modification of the enzyme activity of rat liver supernatant on storage at -20°C, Biochem. J. 108 (1968) 349–351.
[7] E. Della Corte, F. Stirpe, 1972. The regulation of rat liver xanthine oxidase, Biochem. J. 126 (1972) 739–745.
[8] M. Ichikawa, T. Nishino, T. Nishino, A. Ichikawa, Subcellular localization of xanthine oxidase in rat hepatocytes: high-resolution immunoelectron microscopic study combined with biochemical analysis, J. Histochem. Cytochem. 40 (8) (1992) 1097–1103, https://doi.org/10.1177/40.8.1619276.
[9] T. Saito, T. Nishino, Difference in redox and kinetic properties between NAD-dependent and O_2-dependent types of rat liver xanthine dehydrogenase, J. Biol. Chem. 264 (17) (1989) 10015–10022, https://doi.org/10.1016/S0021-9258(18)81761-6.
[10] J. Hunt, V. Massey, Purification and properties of milk xanthine dehydrogenase, J. Biol. Chem. 267 (1992) 21479–21485.
[11] R. Hille, T. Nishino, Flavoprotein structure and mechanism. 4. Xanthine oxidase and xanthine dehydrogenase, Faseb. J. 9 (11) (1995) 995–1003, https://doi.org/10.1096/fasebj.9.11.7649415.
[12] T. Nishino, K. Okamoto, Y. Kawaguchi, T. Matsumura, B.T. Eger, E.F. Pai, T. Nishino, The C-terminal peptide plays a role in the formation of an intermediate form during the transition between xanthine dehydrogenase and xanthine oxidase, FEBS J. 282 (16) (2015) 3075–3090, https://doi.org/10.1111/febs.13277.
[13] J.M. McCord, I. Fridovich, Superoxide dismutase. An enzymic function for erythrocuprein (hemocuprein), J. Biol. Chem. 244 (22) (1969) 6049–6065, https://doi.org/10.1016/S0021-9258(18)63504-5.
[14] N. Cantu-Medellin, E.E. Kelley, Xanthine oxidoreductase-catalyzed reactive species generation: a process in critical need of reevaluation, Redox Biol. 1 (1) (2013) 353–358, https://doi.org/10.1016/j.redox.2013.05.002.
[15] T. Nishino, K. Okamoto, B.T. Eger, E.F. Pai, T. Nishino, Mammalian xanthine oxidoreductase-mechanism of transition from xanthine dehydrogenase to xanthine oxidase, FEBS J. 275 (13) (2008) 3278–3289, https://doi.org/10.1111/j.1742-4658.2008.06489.x.
[16] B.T. Eger, K. Okamoto, C. Enroth, M. Sato, T. Nishino, E.F. Pai, T. Nishino, Purification, crystallization and preliminary X-ray diffraction studies of xanthine Dehydrogenase and xanthine Oxidase isolated from bovine milk, Acta crystallogr. D Biol. Crystallogr. 56 (Pt12) (2000) 1656–1658, https://doi.org/10.1107/s0907444900012890.

[17] L.I. Hart, M.A. McGartoll, H.R. Chapman, R.C. Bray, The Composition of milk xanthine oxidase, Biochem. J. 116 (5) (1970) 851–864, https://doi.org/10.1042/bj1160851.
[18] H.M. Martin, J.T. Hancock, V. Salisbury, R. Harrison, Role of xanthine oxidoreductase as an antimicrobial agent, Infect. Immun. 72 (9) (2004) 4933–4939, https://doi.org/10.1128/IAI.72.9.4933-4939.2004.
[19] C. Vorbach, A. Scriven, M.R. Capecchi, The housekeeping gene xanthine oxidoreductase is necessary for milk fat droplet enveloping and secretion: gene sharing in the lactating mammary gland, Genes Dev. 16 (24) (2002) 3223–3235, https://doi.org/10.1101/gad.1032702.
[20] S. Abadeh, J. Killacky, M. Benboubetra, R. Harrison, Purification and partial characterization of xanthine oxidase from human milk, Biochim. Biophys. Acta 1117 (1992) 25–32.
[21] T. Kusano, D. Ehirchiou, T. Matsumura, V. Chobaz, S. Nasi, M. Castelblanco, A. So, C. Lavanchy, H. Acha-Orbea, T. Nishino, K. Okamoto, N. Busso, Targeted knock-in mice expressing the oxidase-fixed form of xanthine oxidoreductase favor tumor growth, Nat. Commun. 10 (1) (2019) 4904, https://doi.org/10.1038/s41467-019-12565-z.
[22] S.S. Al-Shehri, J.A. Duley, N. Bansal, Xanthine oxidase-lactoperoxidase system and innate immunity: biochemical actions and physiological roles, Redox Biol. 34 (2020), 101524, https://doi.org/10.1016/j.redox.2020.101524.
[23] V.G. Janolino, H.E. Swaisgood, Isolation and characterization of sulfhydryl oxidase from bovine milk, J. Biol. Chem. 250 (7) (1975) 2532–2538, https://doi.org/10.1016/S0021-9258(19)41633-5.
[24] J. Jaje, H.N. Wolcott, O. Fadugba, D. Cripps, A.J. Yang, I.H. Mather, C. Thorpe, A flavin-dependent sulfhydryl oxidase in bovine milk, Biochemistry 46 (45) (2007) 13031–13040, https://doi.org/10.1021/bi7016975.
[25] T. Nishino, T. Nishino, K. Tsushima, Purification of highly active milk xanthine oxidase by affinity chromatography on sepharose 4B/folate gel, FEBS Lett. 131 (2) (1981) 369–372, https://doi.org/10.1016/0014-5793(81)80406-1.
[26] T. Nishino, K. Okamoto, Y. Kawaguchi, H. Hori, T. Matsumura, B.T. Eger, E.F. Pai, T. Nishino, Mechanism of the conversion of xanthine dehydrogenase to xanthine oxidase: identification of the two cysteine disulfide bonds and crystal structure of a non-convertible rat liver xanthine dehydrogenase mutant, J. Biol. Chem. 280 (26) (2005) 24888–24894, https://doi.org/10.1074/jbc.M501830200.
[27] W.R. Waud, K.V. Rajagopalan, Purification and properties of the NAD+dependent (type D) and O2-dependent (type O) forms of rat liver xanthine dehydrogenase, Arch. Biochem. Biophys. 172 (2) (1976) 354–364, https://doi.org/10.1016/0003-9861(76)90087-4.
[28] R.E. Childs, W.E. Bardsley, The steady-state kinetics of peroxidase with 2,2'-azino-di-(3-ethyl-benzthiazoline-6-sulphonic acid) as chromogen, Biochem. J. 145 (1) (1975) 93–103, https://doi.org/10.1042/bj1450093.
[29] M.M. Bradford, A rapid and sensitive method for the quantification of microgram quantities of protein utilizing the principle of protein-dye binding, Anal. Biochem. 72 (1976) 248–254, https://doi.org/10.1006/abio.1976.9999.
[30] M. Morrison, H.B. Hamilton, E. Stotz, The isolation and purification of lactoperoxidase by ion exchange chromatography, J. Biol. Chem. 228 (2) (1957) 767–776, https://doi.org/10.1016/S0021-9258(18)70658-3.
[31] S. Aibara, H. Yamashita, E. Mori, M. Kato, Y. Morita, Isolation and characterization of five neutral isoenzymes of horseradish peroxidase, J. Biochem. (Tokyo) 92 (2) (1982) 531–539, https://doi.org/10.1093/oxfordjournals.jbchem.a133961.
[32] V. Massey, P.E. Brumby, H. Komai, Studies on milk xanthine oxidase. Some spectral and kinetic properties, J. Biol. Chem. 244 (7) (1969) 1682–1691, https://doi.org/10.1016/S0021-9258(18)91738-2.
[33] J.L. Johnson, W.R. Waud, H.J. Cohen, K.V. Rajagopalan, Molecular basis of the biological function of molybdenum. Molybdenum-free xanthine oxidase from livers of tungsten-treated rats, J. Biol. Chem. 249 (16) (1974) 5056–5061, https://doi.org/10.1016/S0021-9258(19)42327-2.
[34] U.K. Laemmli, Cleavage of structural proteins during the assembly of the head of bacteriophage T4, Nature 227 (5259) (1970) 680–685, https://doi.org/10.1038/227680a0.
[35] B.R. Oakley, D.R. Kirsch, N.R. Morris, A simplified ultrasensitive silver stain for detecting proteins in polyacrylamide gels, Anal. Biochem. 105 (2) (1980) 361–363, https://doi.org/10.1016/0003-2697(80)90470-4.
[36] P. Matsudaira, Sequence from picomole quantities of proteins electroblotted onto polyvinylidene difluoride membranes, J. Biol. Chem. 262 (21) (1987) 10035–10038, https://doi.org/10.1016/S0021-9258(18)61070-1.
[37] B.H. Sörbo, Crystalline rhodanese I. Purification and physicochemical examination, Acta Chem. Scand. 7 (1953) 1129–1136, https://doi.org/10.3891/acta.chem.scand.07-1129.
[38] G.L. Ellman, 1959. Tissue sulfhydryl groups, Arch. Biochem. Biophys. 82 (1959) 70–77.
[39] K. Kawakami, K. Yamada, Y. Notsu, M.Z. Hasan, T. Nabika, T. Yamada, Development of one-handed milking device to collect milk from lactating rats: analysis of feeding with the progressive lactation, Shimane J. Med. Sci. 32 (2015) 13–18.
[40] Y. Amaya, K. Yamazaki, M. Sato, K. Noda, T. Nishino, T. Nishino, Proteolytic conversion of xanthine dehydrogenase from the NAD-dependent type to the O_2-dependent type. Amino acid sequence of rat liver xanthine dehydrogenase and identification of the cleavage sites of the enzyme protein during irreversible conversion by trypsin, J. Biol. Chem. 265 (24) (1990) 14170–14175, https://doi.org/10.1016/S0021-9258(18)77283-9.
[41] M.M. Cals, P. Mailliart, G. Brignon, P. Anglade, B.R. Dumas, Primary structure of bovine lactoperoxidase, a fourth member of a mammalian heme peroxidase family, Eur. J. Biochem. 198 (3) (1991) 733–739, https://doi.org/10.1111/j.1432-1033.1991.tb16073.x.
[42] D. Dolman, H.B. Dunford, D.M. Chowdhury, M. Morrison, The kinetics of cyanide binding by lactoperoxidase, Biochemistry 7 (11) (1968) 3991–3996, https://doi.org/10.1021/bi00851a028.
[43] D. Keilin, E.F. Hartree, Purification of horse-radish peroxidase and comparison of its properties with those of catalase and methaemoglobin, Biochem. J. 49 (1) (1951) 88–104, https://doi.org/10.1042/bj0490088.
[44] P.A. Kanthale, D. Lal, R.P. Datir, Establishment of natural levels of thiocyanate in milk of different breeds of cow and murrah breed of buffalo, J. Food Process. Technol. 8 (10) (2017) 698, https://doi.org/10.4172/2157-7110.1000698.
[45] S. Adak, A. Mazumdar, R.K. Banerjee, Low catalytic turnover of horseradish peroxidase in thiocyanate oxidation. Evidence for concurrent inactivation by cyanide generated through one-electron oxidation of thiocyanate, J. Biol. Chem. 272 (17) (1997) 11049–11056, https://doi.org/10.1074/jbc.272.17.11049.
[46] C.M. Harris, V. Massey, The oxidative half-reaction of xanthine dehydrogenase with NAD; reaction kinetics and steady-state mechanism, J. Biol. Chem. 272 (45) (1997) 28335–28341, https://doi.org/10.1074/jbc.272.45.28335.
[47] M.B. Grisham, E.M. Ryan, Cytotoxic properties of salivary oxidants, Am. J. Physiol. 258 (1990) C115–C121, https://doi.org/10.1152/ajpcell.1990.258.1.C115.
[48] P. Nagy, G.N. Jameson, C.C. Winterbourn, 2009, Kinetics and mechanisms of the reaction of hypothiocyanous acid with 5-thio-2-nitrobenzoic acid and reduced glutathione, Chem. Res. Toxicol. 22 (2009) 1833–1840, https://doi.org/10.1021/tx900249d.
[49] M.C. Neville, T.B. McFadden, I. Forsyth, Hormonal regulation of mammary differentiation and milk secretion, J. Mammary Gland Biol. Neoplasia 7 (1) (2002) 49–66, https://doi.org/10.1023/a:1015770423167.
[50] I.H. Mather, T.W. Keenan, Origin and secretion of milk lipids, J. Mammary Gland Biol. Neoplasia 3 (3) (1998) 259–273, https://doi.org/10.1023/a:1018711410270.
[51] W.A. Anderson, J. Trantalis, Y.H. Kang, Ultrastructural localization of endogenous mammary gland peroxidase during lactogenesis in the rat results after tannic acid-formaldehyde-glutaraldehyde fixation, J. Histochem. Cytochem. 23 (4) (1975) 295–302, https://doi.org/10.1177/23.4.47872.
[52] B.Y. Fong, C.S. Norris, A.K.H. MacGibbon, Protein and lipid composition of bovine milk-fat-globule membrane, Int. Dairy J. 17 (4) (2007) 275–288, https://doi.org/10.1016/j.idairyj.2006.05.004.
[53] M.E. Roux, M. McWilliams, J.M. Phillips-Quagliata, P. Weisz-Carrington, M. E. Lamm, Origin of IgA-secreting plasma cells in the mammary gland, J. Exp. Med. 146 (5) (1977) 1311–1322, https://doi.org/10.1084/jem.146.5.1311.
[54] B. Reiter, G. Härnulv, Lactoperoxidase antibacterial system: natural occurrence, biological functions and practical applications, J. Food Protect. 47 (9) (1984) 724–732, https://doi.org/10.4315/0362-028X-47.9.724.
[55] K.D. Kussendrager, A.C. van Hooijdonk, Lactoperoxidase: physico chemical properties, occurrence, mechanism of action and applications, Br. J. Nutr. 84 (2000) S19–S25, https://doi.org/10.1017/s0007114500002208. Suppl. 1.
[56] C. Wijkstrom-Frei, S. El-Chemaly, R. Ali-Rachedi, C. Gerson, M.A. Cobas, R. Forteza, M. Salathe, G.E. Conner, Lactoperoxidase and human airway host defense, Am. J. Respir. Cell Mol. Biol. 29 (2) (2003) 206–212, https://doi.org/10.1165/rcmb.2002-0152OC.
[57] T. Akaike, M. Ando, T. Oda, T. Doi, S. Ijiri, S. Araki, H. Maeda, Dependence on O_2-generation by xanthine oxidase of pathogenesis of influenza virus infection in mice, J. Clin. Invest. 85 (3) (1990) 739–745, https://doi.org/10.1172/JCI114499.
[58] LPO (ENSG00000167419.10) and XDH (ENSG00000158125.9) transcription profile. Retrieved January 4, 2021, from The Broad Institute of MIT and Harvard Web site, https://gtexportal.org/home/gene/, Data Source: GTEx Analysis Release V8 (dbGaP Accession phs000424.v8.p2).
[59] T. Oda, T. Akaike, T. Hamamoto, F. Suzuki, T. Hirano, H. Maeda, Oxygen radicals in influenza-induced pathogenesis and treatment with pyran polymer-conjugated SOD, Science 244 (4907) (1989) 974–976, https://doi.org/10.1126/science.2543070.
[60] R.D. Huff, A.C. Hsu, K.S. Nichol, B. Jones, D.A. Knight, P.A.B. Wark, P.M. Hansbro, J.A. Hirota, Regulation of xanthine dehydrogensase gene expression and uric acid production in human airway epithelial cells, PLoS One 12 (9) (2017), e0184260, https://doi.org/10.1371/journal.pone.0184260.
[61] L. Piccoli, Y.-J. Park, M.A. Tortorici, N. Czudnochowski, A.C. Walls, M. Beltramello, C. Silacci-Fregni, D. Pinto, L.E. Rosen, J.E. Bowen, O.J. Acton, S. Jaconi, B. Guarino, A. Minola, F. Zatta, N. Sprugasci, J. Bassi, A. Peter, A. De Marco, J.C. Nix, F. Mele, S. Jovic, B.F. Rodriguez, S.V. Gupta, F. Jin, G. Piumatti, G. Lo Presti, A.F. Pellanda, M. Biggiogero, M. Tarkowski, M.S. Pizzuto, E. Cameroni, C. Havenar-Daughton, M. Smithey, D. Hong, V. Lepori, E. Albanese, A. Ceschi, E. Bernasconi, L. Elzi, P. Ferrari, C. Garzoni, A. Riva, G. Snell, F. Sallusto, K. Fink, H.W. Virgin, A. Lanzavecchia, D. Corti, D. Veesler, Mapping neutralizing and immunodominant sites on the SARS-CoV-2 spike receptor-binding domain by structure-guided high-resolution serology, Cell 183 (4) (2020) 1024–1042, https://doi.org/10.1016/j.cell.2020.09.037.
[62] Y. Gao, L. Yan, Y. Huang, F. Liu, Y. Zhao, L. Cao, T. Wang, Q. Sun, Z. Ming, L. Zhang, J. Ge, L. Zheng, Y. Zhang, H. Wang, Y. Zhu, C. Zhu, T. Hu, T. Hua, B. Zhang, X. Yang, J. Li, H. Yang, Z. Liu, W. Xu, L.W. Guddat, Q. Wang, Z. Lou, Z. Rao, Structure of the RNA-dependent RNA polymerase from 0COVID-19 virus, Science 368 (6492) (2020) 779–782, https://doi.org/10.1126/science.abb7498.
[63] S. Hati, S. Bhattacharyya, Impact of Thiol−Disulfide balance on the binding of covid-19 spike protein with angiotensin-converting enzyme 2 receptor, ACS Omega 5 (26) (2020) 16292–16298, https://doi.org/10.1021/acsomega.0c02125.
[64] S. De Flora, C. Grassi, L. Carati, Attenuation of influenza-like symptomatology and improvement of cell-mediated immunity with long-term N-acetylcysteine treatment, Eur. Respir. J. 10 (7) (1997) 1535–1541, https://doi.org/10.1183/09031936.97.10071535.

[65] R.I. Horowitz, P.R. Freeman, J. Bruzzese, Efficacy of glutathione therapy in relieving dyspnea associated with COVID-19 pneumonia: a report of 2 cases, Respir. Med. Case Rep. 30 (2020), 101063, https://doi.org/10.1016/j.rmcr.2020.101063.

[66] F. Silvagno, A. Vernone, G.P. Pescarmona, The role of glutathione in protecting against the severe inflammatory response triggered by COVID-19, Antioxidants 9 (7) (2020) 624, https://doi.org/10.3390/antiox9070624.

[67] J.B. Wyngaarden, D.M. Ashton, The regulation of activity of phosphoribosylpyrophosphate amidotransferase by purine ribonucleotides: a potential feedback control of purine biosynthesis, J. Biol. Chem. 234 (6) (1959) 1492–1496, https://doi.org/10.1016/S0021-9258(18)70036-7.

[68] J.L. Smith, E.J. Zaluzec, J.P. Wery, L. Niu, R.L. Switzer, H. Zalkin, Y. Satow, Structure of the allosteric regulatory enzyme of purine biosynthesis, Science 264 (5164) (1994) 1427–1433, https://doi.org/10.1126/science.8197456.

[69] V. Massey, D. Edmondson, On the mechanism of inactivation of xanthine oxidase by cyanide, J. Biol. Chem. 245 (24) (1970) 6595–6598.

[70] N. Pandey, A.K. Singh, M. Sinha, P. Kaur, S. Sharma, T.P. Singh, Crystal Structure of Lactoperoxidase Complexed Simultaneously with Thiocyanate Ion, Iodide Ion, Bromide Ion, Chloride Ion through the Substrate Diffusion Channel Reveals a Preferential Queue of the Inorganic Substrates towards the Distal Heme Cavity, 2010, https://doi.org/10.2210/pdb3NYH/pdb.